LM-04K078
October 14, 2004

Engineering Spectral Control Using Front Surface Filters for Maximum TPV Energy Conversion System Performance

TD Rahmlow, Jr, JE Lazo-Wasem, EJ Gratrix, JJ Azarkevich, EJ Brown, DM DePoy, DR Eno, PM Fourspring, JR Parrington, RG Mahorter, B Wernsman

NOTICE

Engineering Spectral Control Using Front Surface Filters for Maximum TPV Energy Conversion System Performance

Thomas D. Rahmlow[*], Jr, Jeanne E. Lazo-Wasem[†] and Edward J. Gratrix[‡]
Rugate Technologies, Inc

John J. Azarkevich[§], Edward J. Brown[**], David M. DePoy[††], Daniel R. Eno[‡‡],
Patrick M. Fourspring[§§], and, Josef R. Parrington[***]
Lockheed Martin Company

Robert G. Mahorter[†††] and Bernard Wernsman[‡‡‡]
Bechtel Bettis, Inc

Abstract

Energy conversion efficiencies of better than 23% have been demonstrated for small scale tests of a few thermophotovoltaic (TPV) cells using front surface, tandem filters [1, 2]. The engineering challenge is to build this level of efficiency into arrays of cells that provide useful levels of energy. Variations in cell and filter performance will degrade TPV array performance. Repeated fabrication runs of several filters each provide an initial quantification of the fabrication variation for front surface, tandem filters for TPV spectral control. For three performance statistics, within-run variation was measured to be 0.7-1.4 percent, and run-to-run variation was measured to be 0.5-3.2 percent. Fabrication runs using a mask have been shown to reduce variation across interference filters from as high as 8-10 percent to less than 1.5 percent. Finally, several system design and assembly approaches are described to further reduce variation.

I. Introduction

Thermophotovoltaic (TPV) cells provide an effective means of converting above bandgap infrared radiation to electric power. Power conversion efficiency of up to 23% has been demonstrated on a small scale (a few TPV cells) using front surface, tandem filters [1, 2]. The front surface filter reflects below bandgap photons back to the radiator for recuperation, and allows above bandgap photons to pass through into the cell for energy conversion. The emission spectrum from a hot radiator is a function of the radiator's temperature and the wavelength specific emissivity of the radiator's surface. In the example of a blackbody radiator at 950°C and a 0.60 eV bandgap TPV

[*] Vice President, Corporate, 353 Christian Street, Oxford, CT 06478
[†] President, Corporate, 353 Christian Street, Oxford, CT 06478
[‡] Director, Optical Technology, 353 Christian Street, Oxford, CT 06478
[§] Specialist, Advanced Concepts, MS 103, P.O. Box 1072, Schenectady, NY 12301
[**] Sr. Engineer, Advanced Concepts,MS 103, P.O. Box 1072, Schenectady, NY 12301
[††] Lead Engineer, Advanced Concepts, MS 103, P.O. Box 1072, Schenectady, NY 12301
[‡‡] Statistician, Advanced Concepts,MS 103, P.O. Box 1072, Schenectady, NY 12301
[§§]Sr. Engineer, Advanced Concepts, MS 103, P.O. Box 1072, Schenectady, NY 12301
[***] Advisory Scientist, Advanced Concepts, MS 103 P.O. Box 1072, Schenectady, NY 12301
[†††] Engineer, Solid State Materials, P.O. Box 79, West Mifflin, PA 15122
[‡‡‡] Principal Engineer, Solid State Materials, P.O. Box 79, West Mifflin, PA 15122

cell, only about 16% of the incident energy can be converted. The remaining energy, if absorbed within the cell, is lost as heat. By reflecting the below bandgap photons back to the radiator, the filter improves the system efficiency by reducing the amount of energy required to maintain the target radiator temperature.

Figure 1 presents a schematic of a TPV power converter with a front surface filter. Figure 2 presents an overlay of measured spectral reflection for a typical 0.60 eV filter and a normalized blackbody emission spectra for 950 ^{o}C. The filter is a non-polarizing shortpass, broadband reflector. The sharp transition from high transmission to high reflection is placed at the TPV cell's bandgap. The filter is designed to provide good performance at all angles of incidence from near normal to near grazing angles. Figure 3 presents measured reflection for a range of angles.

The filter is a tandem design consisting of a multilayer interference filter deposited onto a plasma filter. The interference filter defines the transition edge and provides high reflection out to about 6.5 microns. The plasma filter provides high reflection from 6 microns to long wavelengths. The plasma filter is a 1 micron layer of InPAs on an InP substrate doped to a nominal density of 5E19/cm^3. Figure 4 presents measured reflection for the plasma filter, the interference filter on silicon, and the tandem filter.

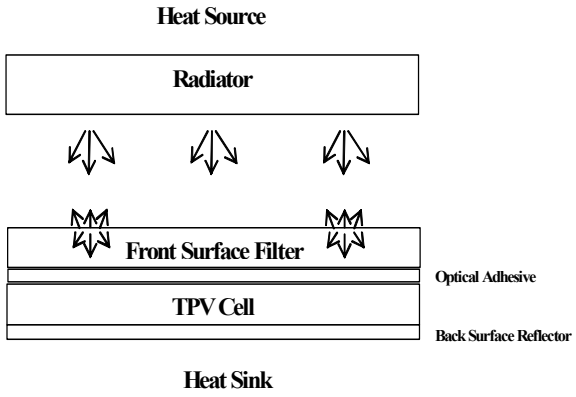

Figure 1. Front surface filters are placed on the cold side of a TPV converter in front of the TPV cell. The filter allows above band gap photons to pass through into the TPV cell and reflects long wavelength photons back towards the source.

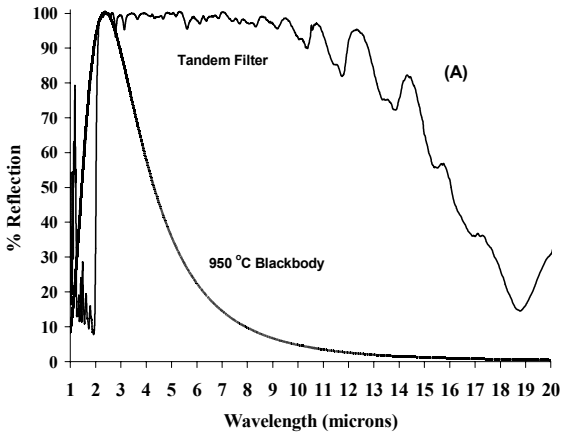

Figure 2. Measured reflection of a front surface tandem filter is plotted along with a black body spectrum for 950 ^{o}C. The filter's transition edge is placed at the cell's band gap. High reflection of below band gap photons is needed to achieve high spectral efficiency.

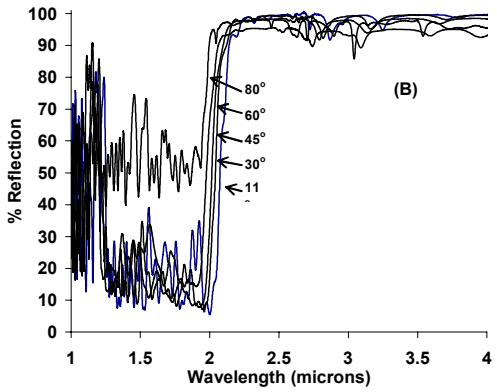

Figure 3. Measured reflection measurements of a 0.6 eV front surface filter highlight the shift in angle of the transition edge with angle of incidence (AOI). The pass band transmission degrades at near grazing angles.

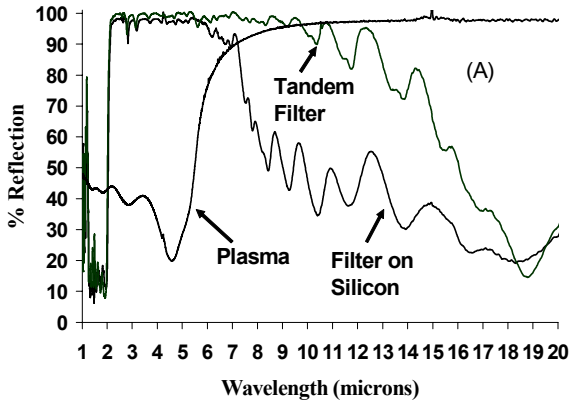

Figure 4. The tandem filter is a multilayer interference filter on a plasma layer InP substrate. Measured reflection of the tandem filter, the plasma filter and interference filter are overlaid.

Spectral efficiency is the ratio of convertible energy that passes through the filter to the total energy absorbed by the filter and cell [3]. Spectral efficiency is a function of both the radiator spectrum and the angle weighted distribution of the flux. The same front surface filter will have a different spectral efficiency for different incident spectra. The spectral efficiency of these designs is calculated from modeled transmission and reflection spectra over the wavelength range of 0.5 to 25 microns at a range of angles from 5 to 85° in increments of 5° and a black body source at 950 °C. The spectral efficiency for fabricated filters is calculated from spectral measurements at 11, 30, 45, 60 and 80° AOI and the calculated performance of a black body source.

The filter designs are developed using angle and energy weighted spectral efficiency and transmission as refinement goals[4]. Spectral efficiency is reduced by absorption in the coating materials. Above bandgap transmission is maximized in order to maximize the power output of the cell. Front surface, tandem filters have achieved the highest spectral performance of any spectral control configuration to date as shown in Figure 5.

While good performance has been demonstrated for small scale TPV modules (1-4 cm^2), developing an array of TPV cells for a larger scale includes a number of engineering and manufacturing issues. Variation in cell and filter performance is a critical concern when assembling an array. Variation due to front surface tandem filters is quantified next.

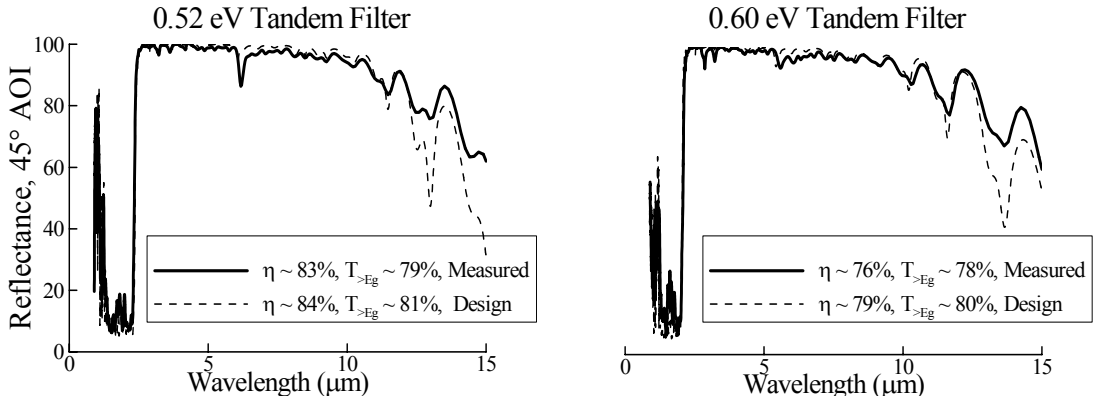

Figure 5. Current Spectral Performance of Front Surface, Tandem Filters for 0.52 eV (a) and 0.60 eV (b) Band Gap TPV Cells. The spectral reflectance at 45° angle of incidence is shown to represent the measured performance of the filters, but the spectral efficiency (η) and above band gap transmission ($T_{>Eg}$) shown in the inset on each figure represent spectrally and directionally weighted values as described in Reference [5]. Assumptions: $T_{radiator}$ = 950°C, T_{cell} = 50°C, $\varepsilon_{radiator}$ = 1.0

II. Characterizing and Improving Filter Performance

Repeated fabrication runs for 0.60 eV and 0.52 eV filters were executed. In each case, the design was fixed and multiple filters per run were fabricated. The 0.60 eV filter runs were tandem filters on 3" InP substrates. Three filters per run were coated in each of 11 runs. The 0.52 eV filter runs were tandem filters on 2" InP substrates. Four filters were coated in each of 12 runs. Two different substrate diameters were used in support of several different TPV development programs. As a result, the data for each substrate diameter were treated as separate numerical populations and are presented separately.

Performance was characterized for variability across a single filter, between filters within a run, and between filters from run to run. Each type of variability has a different assignable cause. Variability across a filter is largely due to the fixtures and geometry of the coating chamber. Filter to filter variations within a run are due to thermal gradients and positioning errors in mounting the part. Run-to-run variations are due to differences in chamber setup, long term drifts in the process or equipment failure during a run.

The specific performance statistics that were used to quantify this variability are defined in Table 1. These statistics characterize edge position, above band gap transmission, and below band gap reflection as a ratio of the measured results to the expected design values, except the across the filter edge statistic. The across the filter edge

statistic represents measured values normalized to the measured value at the center of the filter. Ideally, all the values should be 1.0.

The bases for these performance statistics vary with the statistic and the band gap. First, only measured data at 45° angle of incidence was used as the most complete data set available for all the filters. This angle of incidence is the most important and is expected to represent the actual variability of the filters, but the filters must perform well at all angles of incidence. The analysis of measured spectral performance at additional angles of incidence needs to be completed to fully characterize the filter variability and confirm that the results at 45° angle of incidence represent the actual variability. Second, the transmittance statistic includes measured reflectance beginning at 1.4 µm, and the reflectance statistic includes measured reflectance ending at 10 µm. For a blackbody source at 950°C, about 92 percent of the emitted energy is between 1.4 and 10.0 µm. Third, the transmittance statistic includes measured reflectance ending at 1.9 µm for the 0.60 eV band gap and 2.2 µm for the 0.52 eV band gap, and the reflectance statistic includes measured reflectance beginning at 2.25 µm for the 0.60 eV band gap and 2.5 µm for the 0.52 eV band gap. These values were chosen to exclude the measured data at and near the filter edge, that is the transition from low reflectance to high reflectance. Fourth, the reflectance statistic excludes measured data from 4.15 to 4.50 µm since a known artifact (atmospheric CO_2 absorption) exists within this spectral range. Finally, within the spectral range of 6 µm to 10 µm the reflectance due to the interference filter is decreasing as the reflectance of the plasma layer is increasing. Therefore, the reflectance statistic includes variability from the plasma filter as well as the interference filter. To separate these two sources of variability, the measured reflectance for plasma filters will need to be analyzed and then subtracted from variability indicated by the measured reflectance of the tandem filters.

Table 1 Definitions of the Statistics Used to Quantify Measured Variability

Statistic	**0.60 eV**	**0.52 eV**
Edge	Wavelength position of the 50 percent reflectance of the measured reflectance at 45° angle of incidence.	
Transmittance	Average of measured reflectance at 45° angle of incidence from 1.4-1.9µm	Average of measured reflectance at 45° angle of incidence from 1.4-2.2µm
Reflectance	Average of measured reflectance at 45° angle of incidence from 2.25-4.15; 4.50-10.0µm	Average of measured reflectance at 45° angle of incidence from 2.5-4.15; 4.50-10.0µm

Figure 6 presents overlays of measured reflection from filters taken from all runs. The general features of the filter repeat well from run to run. Measured variability within-run (variability between filters within a fabrication run) and run-to-run are plotted in Figure 7 and are listed in Table 2. The within-run variance and run-to-run variance were estimated for each performance statistic via one-way random effects analysis of variance (ANOVA). The results are summarized in Table 2. The ANOVA results can be considered to quantify the sources of within-run and run-to-run variability. However, for the 0.60 eV filters some of the variability was non-random in nature. In particular, the performance of the first 6 runs for the 0.6 eV data was judged to be low and material tooling factors (rate calibration) were corrected between runs 6 and 7. The result was an improvement in transmission and edge location.

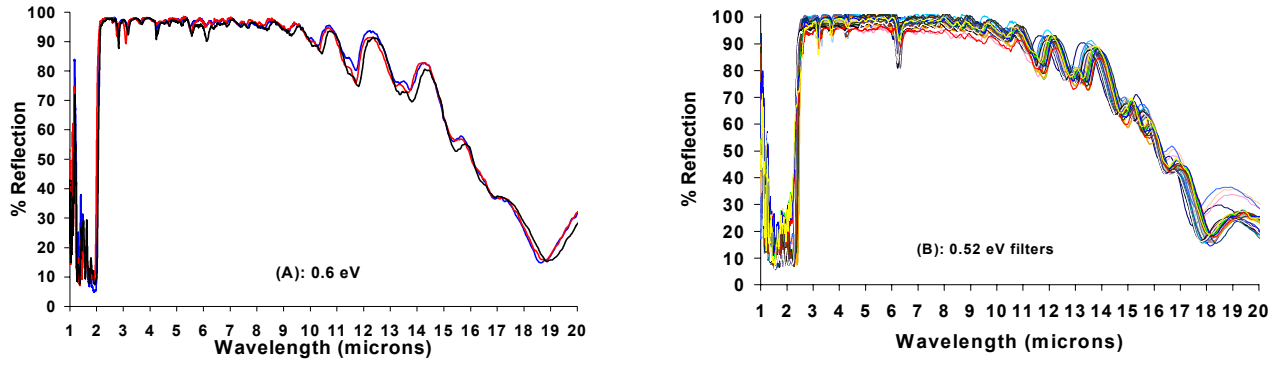

(a) **(b)**

Figure 6. Reflection measured for 0.6 eV filters samples from three runs are overlaid (b). Measurements are at 45° AOI. Measured reflection for all 36 0.52 eV filters are overlaid (a).

Table 2 Summary of Measured Deviations*

Statistic / Factor	**0.60 eV (3 in. dia. wafer)** (%)	**0.52 eV (2 in. dia. wafer)** (%)
Edge		
Across filter without mask	8 - 10	2 - 3
Across filter with mask	< 1.5	< 1.0
Within-run	0.7	1
Run-to-run	1.7	2.8
Transmittance		
Within-run	1.4	0.7
Run-to-run	4.0	0.5
Reflectance		
Within-run	0.5	1.3
Run-to-run	0.4	3.2

* Deviation is the square root of the variance given as a percentage of the mean (in this case 1.0) for the within-run and run-to-run data. For the across filter data, the deviation is given as a percentage of the measured value at the center of the wafer.

For most cases, the run-to-run deviation is greater than the within-run deviation. Therefore, additional process improvements should focus on reducing the run-to-run deviation further.

Uniformity varied 8 to 10 % from one edge of a filter to the other, without a deposition mask. Figure 8 presents a plot of radial variation in edge position across the 3" parts for filters fabricated in the first set of 0.6 eV filter runs. The parts are held in a platen that rotates throughout the deposition. Performance varies across the filter in the direction that corresponds to the radius of the rotation of the tool.

A deposition uniformity mask blocks a portion of the coating area from the source. Uniformity is achieved by shaping the mask to block more or less of a region. The uniformity mask is designed from the geometry of the chamber and the plume characteristics of the sources. A static rate field is first calculated. The shadow of the mask and obstructions are then projected onto the rate field. Deposition is modeled by 'moving' the part through the rate field and summing the product of the dwell time and rate at each point. The mask design is iterated to minimize the radial non-uniformity across the part. Figure 9 presents a contour plot of the static rate field calculated for the chamber geometry and the computer generated deposition mask.

Figure 10 presents a plot of measured uniformity across 3" interference filters[§§§] prior to using a mask and after the mask was added. The third plot in this figure presents results of a final iteration in the mask design. Non-uniformity across the part dropped from 10% edge to edge to about 2% with the first iteration of the mask and to about 1.2% after the second iteration.

The level of variability resulting from the fabrication can be mitigated through system design and assembly techniques as discussed next.

[§§§] The filters used to develop the mask are the interference filter portion only of the tandem filter. Glass substrates were used rather than the InP substrates with the epitaxially deposited plasma layer necessary to complete the tandem filter.

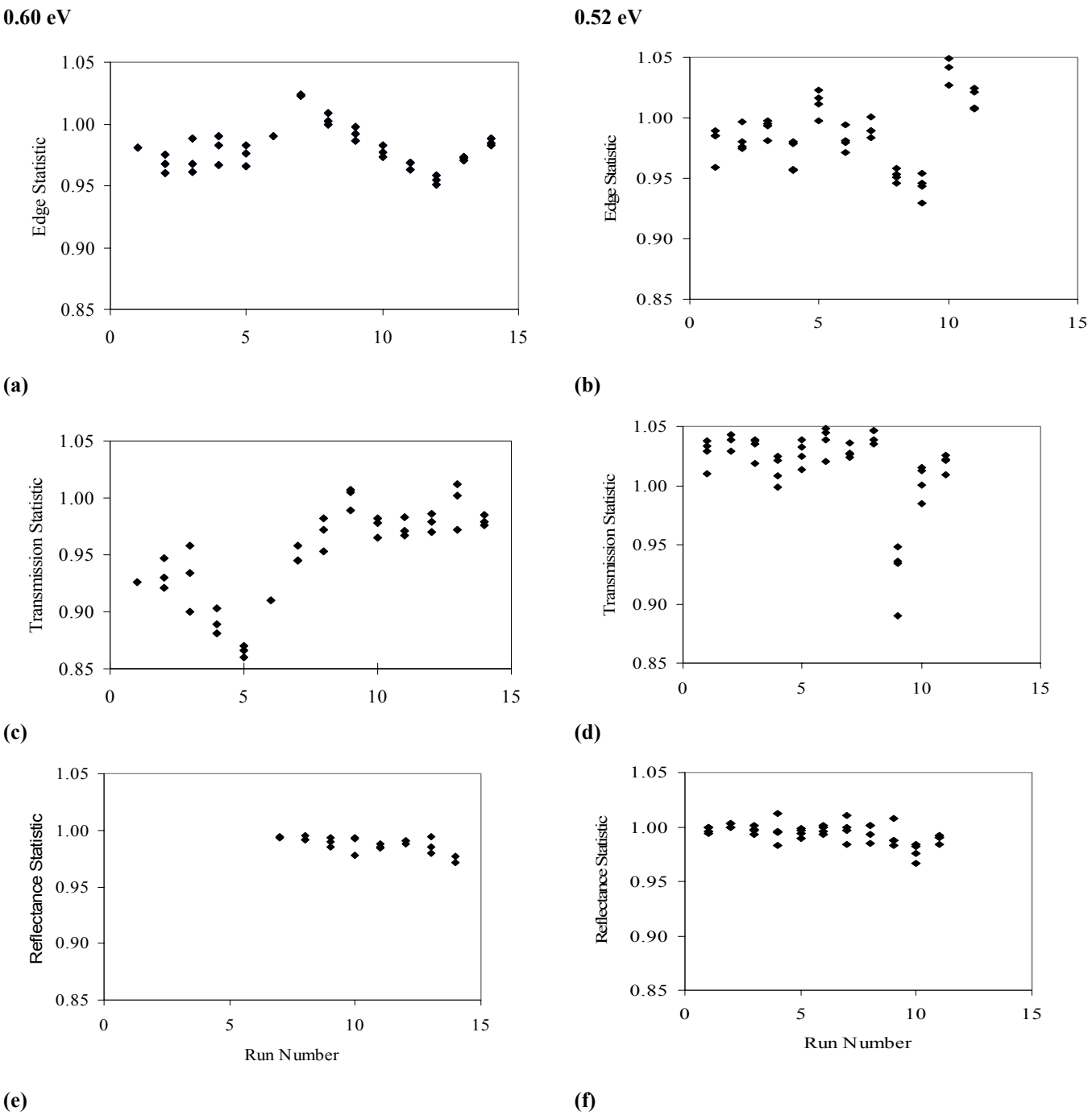

Figure 7. Measured Variability Within-run and Run-to-run for Three Relevant Statistics

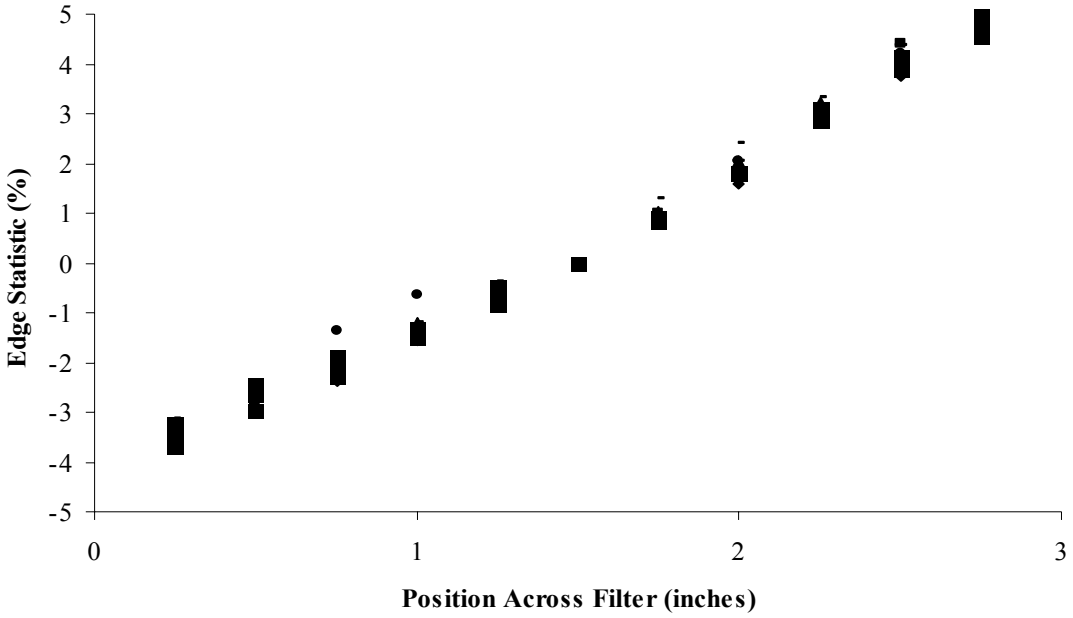

Figure 8. Edge performance statistic measured across an initial set of 10 tandem filters (3 inch diameter) showing 8 to10 % variability as the result of chamber geometry.

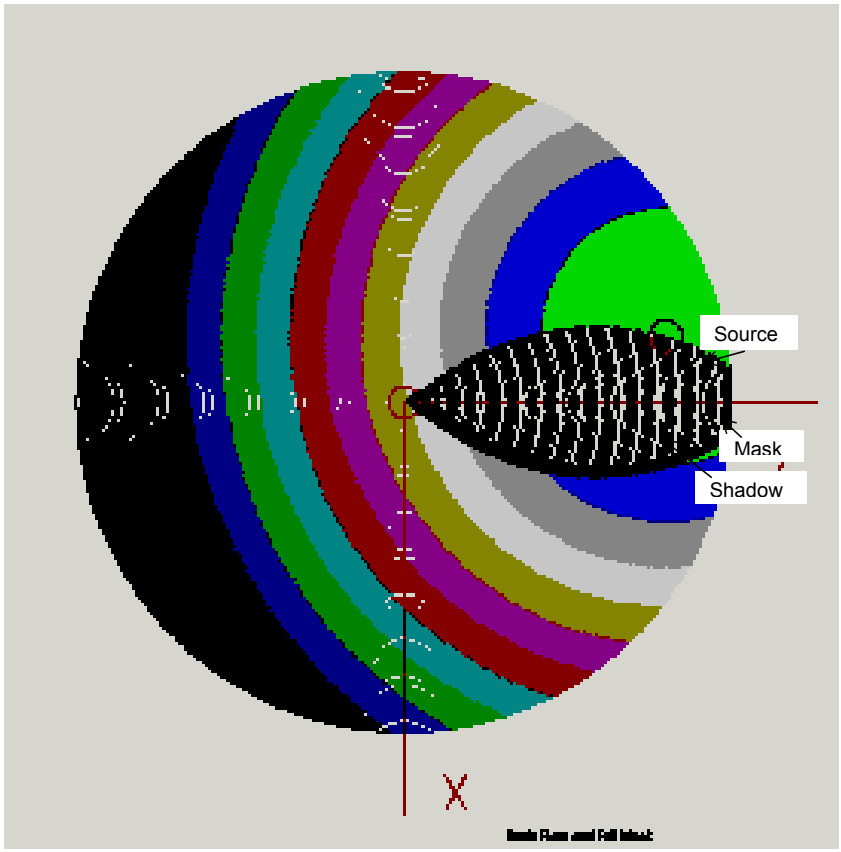

Figure 9. The modeled static flux from the high index source is plotted as contours along with the computer generated deposition mask and the shadow of the mask projected onto the coating plane.

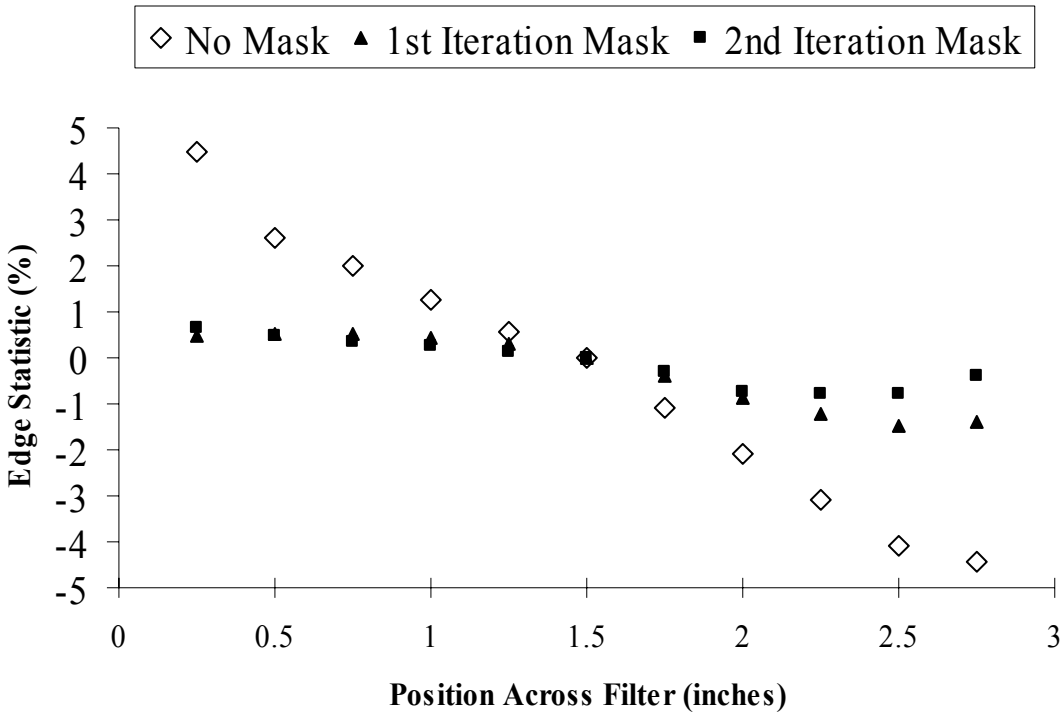

Figure 10. Edge performance statistic as a function of position across 3 inch diameter interference filters showing the reduction of non-uniformity from 10% to 1.2%.

III. System Design and Assembly

The front surface, tandem filters should be selected and arranged to support the design of the underlying TPV array.

In general, the TPV array design will use current matched, series connected strings arranged in parallel to build the necessary voltage [6]. Therefore, the front surface, tandem filters should be sorted on above band gap transmission [5] and assembled to align with the underlying strings. This approach will insure the photons reaching the strings will be as uniform as possible and thus minimize current mismatch.

The filters are deposited on circular wafers, but to enhance power density TPV arrays are expected to require square, rectangular, or hexagonal shaped filters. Therefore, the tandem filters need to be cut without damaging the multilayer, interference filter portion of the filter. To date, two general approaches have been used successfully, scribing and cleaving and dicing.

Scribing and cleaving involves scoring lines on the filter to determine the final shape and then breaking (cleaving) the filter along these lines to obtain the desired, final shape. Dicing refers to a sawing procedure to obtain the desired, final shape. A comparison of these two approaches is shown in Figure 11. This comparison suggests that the dicing approach provided a better, less ragged edge. Many issues exist with either approach, and additional development and study of both approaches are required to insure that the best approach is identified for processing tandem filters.

In addition, reducing the length of edge, regardless of quality, per unit area will reduce parasitic absorption at the filter level of the system. Larger wafers and hence larger tandem filters reduce the length of edges and thus provide an advantage over tandem filters fabricated on smaller wafers.

Finally, the filter edges should fall between active regions of the TPV cells to maximize the light incident on the regions of the TPV cells that produce power.

The tandem filters are attached to the front surface of the TPV cells using an optical adhesive. Optical profilometry data can be used to ascertain the flatness of the TPV array so that the quantity of optical adhesive can be adjusted to compensate and thus reduce variation in the flatness of the resulting TPV array.

The tandem filters are attached to the front surface of the TPV cells using an optical adhesive. Optical profilometry data can be used to ascertain the flatness of the TPV array so that the quantity of optical adhesive can be adjusted to compensate and thus reduce variation in the flatness of the resulting TPV array.

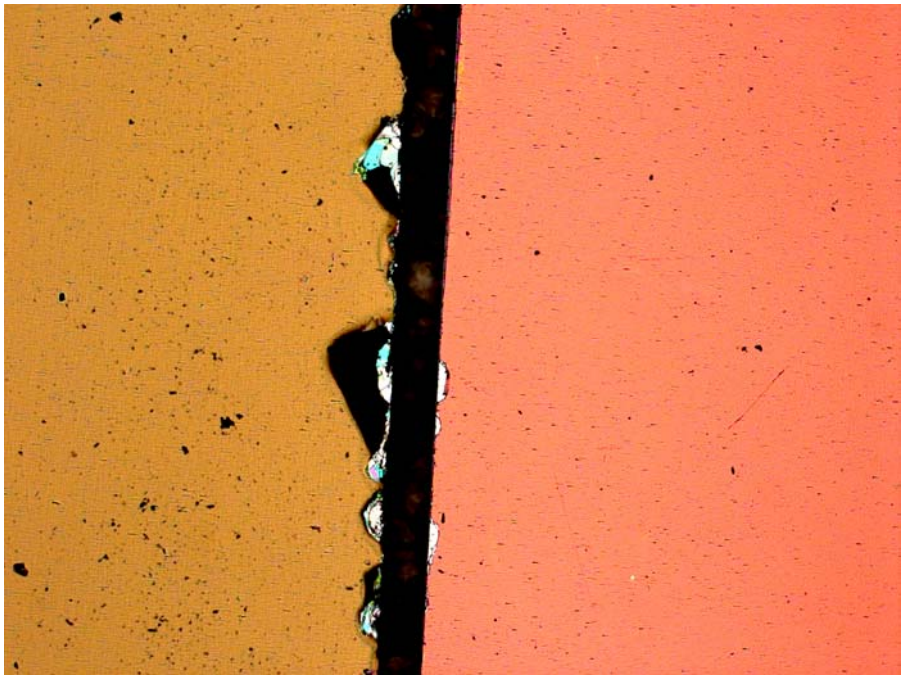

Scribed and Cleaved Edge ↑ **↑ Diced Edge**

Figure 11. Edge Comparison of a Scribed/Cleaved and a Diced Tandem Filter (50X Magnification)

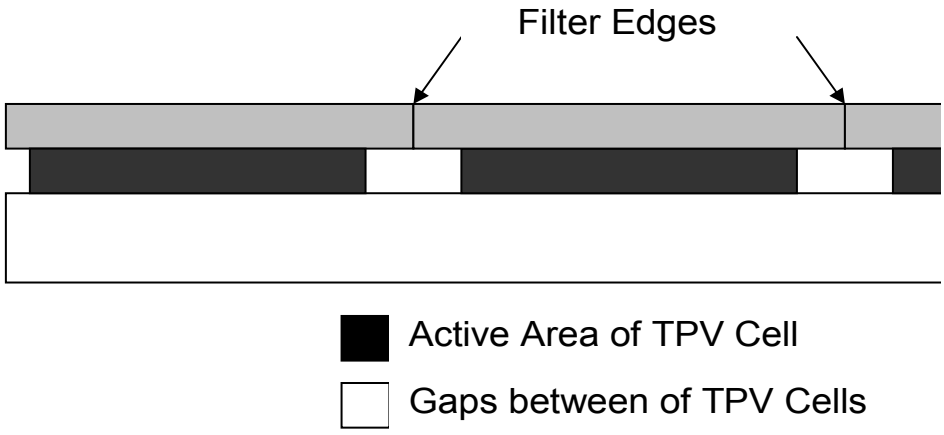

Figure 12. Filter Edge Location Relative to the Active Area of the TPV Cells

IV. Conclusions

Repeatable fabrication of complex tandem filters for TPV spectral control has been demonstrated for two different band gaps with over 24 runs resulting in more than 75 filters. Fabrication variation of front surface, tandem filters has been quantified for the first time. For three performance statistics, within-run variation was measured to be 0.7-1.4 percent, and run-to-run variation was measured to be 0.5-3.2 percent. These are the results for all the filters attempted to be fabricated. Fabrication runs using a mask have been shown to reduce variation across interference filters from as high as 8-10 percent to less than 1.5 percent.

V. References

1. Wersmann, B et. al Greater than 20% Radiant Heat Conversion Efficiency of a Thermophotovoltaic Radiator Module Using Reflective Spectral Control. IEEE Transactions on Electron Devices, 2004. 51(3): 512-515.
2. Wanlass, M, Recent Advances in Low-Bandgap, InP-Based GaInAs/InAsP Materials and Devices for Thermophotovoltaic (TPV) Energy Conversion, TPV 6 Proceedings (in print)
3. Baldasaro, P.F. et al., Thermodynamic Analysis of Thermophotovoltaic Efficiency and Power Density Tradeoffs. Journal of Applied Physics, 2001, 89: p. 3319-3327
4. Rahmlow, T, et al., New Performance Levels for TPV Front Surface Filters, TPV 6 Proceedings (in print), AIP.
5. Talamo, P, TPV Spectral Control, TPV 6 Proceedings (in print)
6. Baldasaro, P., System Performance Projections for TPV Energy Conversion, TPV 6 Proceedings (in print)